Journal of Molecular Structure 1203 (2020) 127461

Contents lists available at ScienceDirect

Journal of Molecular Structure

journal homepage: http://www.elsevier.com/locate/molstruc

Intricate spectroscopic profiling, light harvesting studies and other quantum mechanical properties of 3-phenyl-5-isooxazolone using experimental and computational strategies

Y. Sushma Priya [a], K. Ramachandra Rao [b], P.V. Chalapathi [c], A. Veeraiah [d], Katta Eswar Srikanth [d], Y. Sheena Mary [e], Renjith Thomas [f, *]

[a] Department of Physics, Adikavi Nannaya University, Rajamahendravaram, Andhra Pradesh, India
[b] Department of Physics, Government College, Rajamahendravaram, Andhra Pradesh, India
[c] Department of Physics, Jawaharlal Technological University, Chilakaluripet, Andhra Pradesh, India
[d] Molecular Spectroscopy Laboratories, Department of Physics, D.N.RCollege (A), Bhimavaram, Andhra Pradesh, India
[e] Department of Physics, Fatima Mata National College (Autonomous), Kollam, Kerala, India
[f] Department of Chemistry, St Berchmans College (Autonomous), Changanassery, Kerala, India

ARTICLE INFO

Article history:
Received 13 October 2019
Received in revised form
13 November 2019
Accepted 20 November 2019
Available online 23 November 2019

Keywords:
DFT
FT-IR
FT-Raman
NMR
LHE
NLO
DSSC
Docking

ABSTRACT

This manuscript presents the detailed experimental and computational structural, physical property study of 3-phenyl-5-isooxazolone (3P5I). Different experimental spectral studies like IR, UV, Raman and NMR were used to get an insight on the actual structure of the compound. |It was followed by computational simulation of the structure using DFT approach employing B3LYP functional and 6-311++G (d, p) basis set. Scaled quantum mechanical force field method (SQMFF)was used to assign different vibrations in the spectra using normal coordinate analysis (NCA) and found that close agreement with investigational values. Experimental NMR(^{1}H and ^{13}C NMR) spectrum was also compared with the theoretically simulated spectra using GIAO-gauge independent atomic orbital formalism. UV −Vis Spectrum of compound also studied extensively using theoretical and experimental techniques. Most importantly, the compound shows high light harvesting efficiency hence can be used like a very good photosensitiser in DSSC (dye sensitized solar cells). The overall efficiency of the cell is more than 8% in a titanium dioxide based cell, which is high when compared to similar cells. MEP surfaces, HOMO-LUMO, NLO properties, chemical reactivity descriptors, NBO analysis, and Mulliken atomic charge analysis were also executed to predict physical as well as chemical properties. Molecular docking simulations show that the compounds can be used as effective apoptosis agonist and antiasthmatic agent.

1. Introduction

Heterocyclic compounds involving oxygen and/or nitrogen have diverse applications, particularly in biology, medicine, and chemistry. Oxazolone is a five-membered heterocyclic compound also referred to as Oxazol-5-(4H)-one. Owing to their various reactive sites, Oxazolonesare having extensive applications in biology, pharmacy and chemical sciences. Further, 5(4H)-oxazolones enormous class of π-conjugated substances, possessing implicit applications in photonicsas well as in electronics; have additionally been read for nonlinear optical properties [1]. Oxazolones are key precursors for synthesis of biosensor couplingnon-natural amino acids, amino alcohols, and heterocyclic molecules. The derivatives of oxazolone compounds found to have NLO properties in solids and solutions [2,3]. With the substitution of the phenyl ring at the third position ofisooxazolone ring makes oxozolone suitable for applications in electronics and photonics. There have been numerous studies reported regarding the spectroscopy and nonlinear optical properties of the oxazolone [4–9].

In this paper, we characterize and describe the structural parameters, vibrational parameters and Chemical shiftsof 3-phenyl-5-isooxazolone, both theoretically and experimentally. Moreover, to analyze the geometrical parameters of the 3P5I compound Natural bond analysis (NBO) was executed. DFT approachbe performed by B3LYP method using6-311++G(d,p) high level basis set. Inthe current investigation, we report the vibrational analysis of 3-

* Corresponding author.
E-mail address: renjith@sbcollege.ac.in (R. Thomas).

https://doi.org/10.1016/j.molstruc.2019.127461
0022-2860/

phenyl-5-isooxazolone (3P5I)using the method of SQM force field. From the predicted Raman and IR intensities, simulated Raman and IR spectra are plotted. Experimental data is observed to be well compared with theoretical data calculated from quantum mechanical methods. Hence, current study was made to investigate entire vibrational spectra of 3P5I in addition to recognize different modes with prominent wave length precession. The experimental (^{1}H and ^{13}C) NMR spectrum was compared with theoretical simulated NMR spectra of 3P5I compound using gauge-independent atomic orbital (GIAO) formalism. Prominently the high light harvesting efficiency of the compound shows that 3P5I can be used as a very good photosensitiser in dye sensitized solar cells. A comparative experimental and theoretical spectra were carried out to measure the basic chemical shifts and show a good agreement. The electronic properties such asNLO properties, Molecular Electrostatic Potential, Mulliken atomic charges, chemical activity descriptors and HOMO-LUMO energy separation were studied and reported. The docking studies show that the compound can be used as antiasthmatic agent.

2. Investigational methods

2.1. FT infrared and Raman spectrum

The FTIR spectrum of 3P5I molecule was determined in the range 4000–400 cm^{-1}by Spectrum GX Fourier transform spectrometer fitted with IR Nicolet microscope and KBr beam splitter by powder method at ±1 cm^{-1} resolution. Fourier transform Raman spectrum of 3P5I was calculated using Nicolet Magna 750 Raman spectrometer at 4 cm^{-1}resolution in range 4000-400 cm^{-1} equipped with an InGaAs detector. Neodymium: Yttrium Aluminum Garnet laser (1064 nm line and typical laser power of 500 mW) excitation source.

2.2. UV–vis spectrum

Ultraviolet–Visible spectrum of 3P5I was traced in the range200–400 nm with Lambda 35 UV–Vis spectrometer (PerkinElmer) with a resolution of 0.05 nm–4.0 nm. UV data were recorded, with a period of 1 nm after 1 cycle, a slit width of 2 nm using dimethyl sulfoxide as a solvent at a scan rate of 240 nmmin^{-1}.

2.3. NMR spectrum

^{1}H (proton) and ^{13}C (neutron)Nuclear Magnetic Resonance spectrum of 3P5I was graphically noted with Bruker spectrometer 400-MHz a sppm (parts per million). The Experimental chemical shifts were found using dimethyl sulfoxide (DMSO) as a solvent.

3. Computational details

Gaussian 09 W Revision- D.01 [10] program was used for doing computational studies. The optimizations were performed with the guess geometry and frequency calculations assured that here are no imaginary frequencies and the molecule represents a global minima. DFT approach used for all computations with B3LYP level 6-311++G (d, p) high level set. Assuming molecular point group symmetry (Cs) the cartesian hypothetical force constants were noticed for the optimized molecular geometry. By MOLVIB 7.0 program [11,12], conversion of Cartesian force field into internal coordinates followed by scaling, the consequent normal coordinate analysis(NCA) by PED matrix and IR, Raman intensities were performed. To understand stabilization energy of the molecule NBO program version 3.1 was performed on Gaussian 09 W Revision- D 0.1 package at DFT approach B3LYP level.

The calculated Raman activities by the GAUSSIAN-09W Revision- D 0.1program and adjusted during scaling by MOLVIB7.0 program then altered to Raman intensities by the formula

$$I_i = \frac{f(\nu_0 - \nu_i)^4 S_i}{\nu_i[1 - \exp[\frac{-hc\nu_i}{kT}]]} \quad (1)$$

ν_o is exciting frequency (cm^{-1}), ν_i is vibrational wave number of the normal mode, h, c, and k are universal constants and f is properly chosen normalization factor used for whole Raman intensities. TD-DFT calculations with CAM-B3LYP functional with 6–311++G(d,p) basis set was used to simulate electronic spectra of 3P5I compound in addition to study the further light harvesting properties.

4. Results and discussions

4.1. Optimized structure

Optimized structure of 3P5I was represented in Fig. 1. The optimized geometrical parameters of 3P5I were calculated theoretically from the DFT/B3LYP method tabulated in Supplementary material 1. The theoretical optimized parameters compared with experimental parameters by atomic numbers provided at Fig. 1. While Experimental crystal data of 3P5I is not presented, Experimental data of the reference molecule 5-dihydroisoxazol-3-yl]-1-methylpyridinium iodide–4-[3-(4-fluorophenyl) - 2-methyl-5-oxo-2, 5-dihydroisoxazol-4- yl]-1-methylpyridinium iodide [13] was taken for comparison. Moreover, we identified that the bond length deviations were more for the bond C-H and less for the bonds N-O,N-C, C-C, and C-O. There is an exact theoretical and experimental equivalence for the O11-N10 bond length. The deviation for the bond length varies from 0 to 0±0.136 Å. Bond angle deviation was maximum for the bond angle C8-C9-O12. These deviations may be caused because the theoretical calculations of the 3P5I were executed in the gas phase while investigational calculations were done in the solid state. The global minimum energy from DFT approach to this optimized structure was-548.6516376 hartrees.

4.2. Molecular vibrations

The title compound 3P5I is a nonlinear molecule having 19 atoms with Cs symmetry with 51 normal mode internal vibrations and these were spread among the symmetry species by the

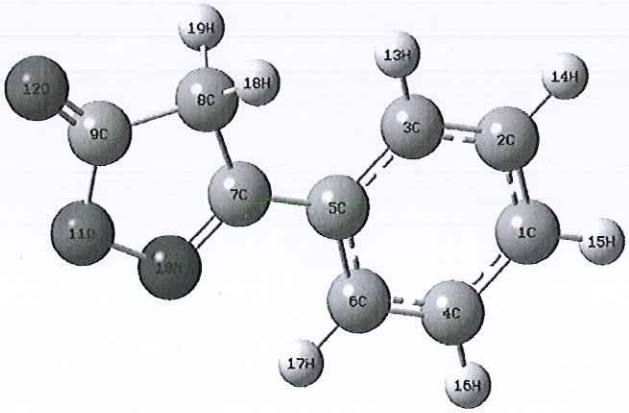

Fig. 1. Optimized geometry structure of 3-phenyl-5-isooxazolone with atomic numbers.

equation

$\Gamma 3N-6 = 35\text{inplane} + 16\text{outofplane}$

Total vibrations were active in Raman and IR.

The task of assigning vibrational frequencies was done by NCA-normal coordinate analysis. 76 internal coordinates were identified and included at supplementary material 2. We constructed non-redundant local symmetry coordinates as listed in Table 1 from the guidelines of author Fogarasi [14,15]. Latter computed force fields from DFT method were transformed to the vibrational co-ordinates. The complete fundamental vibrations were included in Table 2. Through proper scaling graphical comparison between theoretical and experimental FT-IR and FT-Raman spectra are visualized within Figs. 2 and 3. The RMS error between the practical and simulated frequencies after scaling is found to be 2.61 cm^{-1}.

4.3. Vibrational analysis

4.3.1. Carbon-hydrogen vibrations

The theoretical symmetric C-H vibrations observed at 3221,3211,3201,3192 and 3185 cm^{-1} were assigned to C1-H15, C2-H14, C3-H13, C4-H16, and C6-H17 respectively. C-H bending (in plane)vibrations were noticed at frequency range 1700-1000 cm^{-1} A strong infrared band noticed at 1561 cm^{-1} further very strong Raman peak at 1558 cm^{-1} were allocated to in-plane C-H bending vibrations. Moreover, strong infrared peak at 1448 cm^{-1} correspondingly very weak Raman peak at 1441 cm^{-1} was allocated to in-plane C-H bending vibration. Strong infrared peak noticed at 1169 cm^{-1} was allocated to in plane bending C-H vibration. The C-H out of plane bending vibrations emerges between 675 and 1000 cm^{-1}region [16,17]. However strong Raman peak observed at 993 cm^{-1} in addition to very strong peak noticed at 765 cm^{-1}were allocated to C-H bending vibration (out of plane).

4.3.2. Methylene group frequencies

The experimental symmetric stretching vibrations noticed in IR &Raman spectra by 3069, 3065 cm^{-1} was allotted to scaled theoretical frequency at 3076 cm^{-1}. The bands for scissoring, wagging, rocking and twisting CH2 group vibrations listed in Table 1. Those assignments are assisted by PED distribution.

4.3.3. Ring vibrations

In the existed investigation a strong Infrared band noticed at 1080 and 638 cm^{-1} were allocated to ring bending (in-plane) modes. Strong IR peak noticed at 543 cm^{-1} was allocated to ring bending mode (out of plane) vibration. Those small variations in frequency values noticed for these modes are because of variations in reduced mass ratio or force constant.

The bands corresponding to Ring 2 mixed stretching Carbon–Carbon vibrations noticed at scaled frequency 1399 and 894 cm^{-1} were allocated to a very strong experimental IR peak at

Table 1
Definition of local-symmetry coordinates and the values of corresponding scale factors used to correct the B3LYP/6-311++ G (d, p) force field calculations of **3-phenyl-5-isooxazolone**

No.(i)	Symbol[a]	Definition[b]	Scale factors
Stretching			
1–6	ν(C-C) R1	R1, R2, R3, R4, R5, R6	0.999
7–8	ν(C-C) R2	R7, R8,	0.999
9	ν(C-C)	R9	0.999
10–14	ν(C-H) R1	R10, R11, R12, R13, R14	0.999
15	ν(C-H) SS	(R15 + R16)/√2	0.999
16	ν(C-H) AS	(R15-R16)/√2	0.999
17–18	ν(C-O)	R17, R18	0.999
19	ν(C-N)	R19	0.998
20	ν(N-O)	R20	0.997
In-Plane bending			
21	β R1 tri	(γ 21-γ 22+ γ23-γ 24+ γ25-γ26)/√6,	0.998
22	β R1 asy	(2γ 21-γ 22- γ23+2γ24- γ25-γ26)/√12,	0.997
23	β R1 sym	(γ 22 γ23+ γ25-γ26)/2,	0.999
24	β R2 asy	(a-b) (γ28- γ31) +(a+b) (γ29- γ30)	0.999
25	β R2 sym	γ 27 + a(γ28+ γ31)-b (γ29+ γ30)	0.995
26–30	β(C-C-H) R1	(γ32-γ33)/√2, (γ34-γ35)/√2, (γ36-γ37)/√2, (γ38-γ39)/√2, (γ40-γ41)/√2	0.999
31	βC-C-O	(γ42-γ43)/√2	0.996
32–33	β CCC sub	(γ44 −γ45)√2, (γ46 −γ47)√2	0.997
34	βCOCl sc	(γ48 + γ49 + γ50 + γ51)/2	0.998
35	βCOCl ro	(γ48 + γ49 - γ50 - γ51)/2	0.999
36	βCOCl wa	(γ48 - γ49 + γ50 - γ51)/2	0.998
Out of plane bending			
37–41	ω (C-H)	ρ 52, ρ 53, ρ 54, ρ 55, ρ 56	0.997
42	ω (C-O)	ρ 57	0.990
43–44	ω (C-N)	ρ 58, ρ 59	0.999
Torsion			
45	τ R1tri	(τ 60-τ61+τ62-τ63+τ64- τ65)/√6	0.999
46	τ R1asy	(τ 60-τ62+τ63-τ65)/2	0.999
47	τ R1sym	(-τ60-2τ61-τ62+τ63+2τ64-τ65)/√12	0.963
48	τ R2asy	- b(τ66+τ70)+a(τ67+τ69)+τ68	0.999
49	τR2sym	(a-b)(τ69- τ67)+(1-a) (τ70- τ66)	0.975
50	τ Butter	(τ 71 + τ 72 + τ 73 +τ 74)/2	0.997
51	τ COCl	(τ 75 - τ 76)/2	0.999

Where a = cos144°, b = cos72°.
Abbreviations: ν, stretching; β, in plane bending; ω, out of plane bending; τ, torsion, ss, symmetrical stretching, ass, asymmetrical stretching, sc, scissoring, wa, wagging, tw, twisting, ro, rocking, tri, trigonal deformation, sym, symmetrical deformation, asy, asymmetric deformation, butter, butterfly, ar, aromatic, sub, substitution.
[a] These symbols are used for description of the normal modes by PED.
[b] The internal coordinates used here are defined in table given in supplementary material 2.

Table 2
Detailed assignments of fundamental vibrations of 3-phenyl-5-isooxazolone by normal mode analysis based on SQM force field calculations using B3LYP/6-311G++ (d,p).

Mode No.	FT-IR		Activity		Assignments (PED)[a,b]
	Experimental frequencies (cm^{-1})	Theoretical frequencies (cm^{-1})	IR[d]	RAMAN[c]	
7	–	3221	0.0054	34.96	υ CH (99)
8	–	3211	0.0112	57.83	υ CH (99)
9	–	3201	0.5218	19.49	υ CH (99)
10	–	3192	0.2092	31.72	υ CH (99)
11	–	3185	0.0002	7.68	υ CH (99)
12	–	3116	0.04	13.54	υ CH2as (100)
13	3069 w	3076	0.0966	20.92	υ CH2ss (88)
14	2035 vw	1902	0.0006	5.12	υ CCR2 (39), υ CO (35), β R2asy (25)
15	–	1663	0.0697	18.02	υ CCR1 (39), β R2asy (16), υ CN
16	–	1652	0.0782	100	υ CN (31), β R2asy (28), υ CCR1 (16)
17	–	1620	0.0019	56.14	υ CN (37), υ CCR1 (20), β R2asy (16)
18	1561 s	1544	0.0007	5.16	β CH(35), υ CCR1(22),υCCR2(18),βR2asy(17)
19	1448 s	1489	0.0347	6.47	β CH (40), υ CCR1 (28)
20	–	1440	0.0195	2.55	β R2asy (39), υ CCR2 (30), β CH2sc (29)
21	1359 vs	1399	0.0002	19.08	υ CCR2 (54), β R2asy (36)
22	–	1367	0.0001	1.40	υ CCR1 (53), β CH (30)
23	–	1340	0.0095	0.11	υ CCR1 (39), β CH (28), υ CCR2 (18)
24	–	1242	0.0009	20.57	υ CCR2 (57), β CH2wa (25)
25	–	1210	0.0014	3.59	β CH (76), υ CCR1 (19)
26	1169 vs	1190	0.0166	2.79	β CH (78), υ CCR1 (16)
27	–	1175	0.009	0.35	β R2asy (72), υ CCR2 (17)
28	–	1152	0.016	61.74	τ CH2 (85)
29	–	1113	0.0033	0.24	υCCR1(30), βCH (25),β R2asy (20),υCCR2(15)
30	1080 s	1066	0.0054	0.79	β R2asy (49), υ CCR2 (32)
31	–	1043	0.0112	3.29	β R2asy (49), υ CCR2 (29)
32	–	1016	0.5218	11.0	β R1tri (64), υ CCR1 (34)
33	–	1009	0.2092	0.18	ω CH (83)
34	–	982	0.0002	0.01	ω CH (91)
35	–	971	0.04	0.45	β CH2Ro (41), ω CC (16), ω CH (15)
36	–	936	0.0966	0.36	ω CH (79)
37	910 s	928	0.0006	0.59	υ NO (62), β R2asy (33)
38	876 vs	894	0.0697	6.60	υ CCR2 (37), β R2asy (23), υ NO(20),υCO(17)
39	–	860	0.0782	1.42	ω CH (100)
40	–	856	0.0019	0.45	υ CCR2 (78)
41	765 vs	779	0.0007	0.14	ω CH (48), τ R1tri (33), ω CC (15)
42	–	736	0.0347	1.29	υ CO (19),β R2asy (18), υNO(16),β R2sym (16)
43	–	706	0.0195	0.29	τ R1tri (62), ω CH (31)
44	–	654	0.0002	0.84	υ NO (69)
45	638 s	631	0.0001	1.96	β R1asy (57), β R1sym (24)
46	543 s	575	0.0095	0.14	τ R2sym (33), ω CC (28), ω CO (23)
47	–	539	0.0009	1.53	β R2asy(48)
48	–	527	0.0014	0.35	ω CO(22), ωCC(20)
49	–	441	0.0166	0.16	τ R2sym(29), ωCC(17)
50	–	411	0.009	0.01	τ R1sym (52), τ R1asy (29), ω CH (16)
51	–	391	0.016	0.14	β R2asy (70), υ NO (17)
52	–	320	0.0033	0.16	τ R2sym (36), τ CH2 (20), τ R1asy (19)
53	–	315	0.0054	1.33	β R2asy (53), υ CCR2 (32)
54	–	162	0.0112	1.12	τ R2asy(36), τ R2sym(18)
55	–	133	0.5218	0.02	β R2asy(60), υ NO (16)
56	–	85	0.2092	0.35	ω CC (30), τ R2asy (28), τ R2sym(16)
57	–	44	0.0002	0.50	τ CCCC (80), τ R2asy

[a] Only PED contributions ≥15% are listed by DFT method.
[b] Abbreviations: υ, stretching; β, in plane bending; ω, out of plane bending; τ, torsion, ss, symmetrical stretching, as, asymmetrical stretching, sc, scissoring, wa, wagging, twi, twistivg, ro, rocking, ipb, in-plane bending, opb, out-of -plane bending; tri, trigonal deformation, sym, symmetrical deformation, asy, asymmetric deformation, butter, butterfly, ar, aromatic, sub, substitution, vs, very strong; s, strong; ms, medium strong; w, weak; vw, very weak.
[c] Relative Raman intensities calculated by Eq. (1) and normalized to 100.
[d] Relative absorption intensities normalized with highest peak absorption equal to 1.

1359 and 876 cm^{-1} correspondingly. Similarly, weak experimental Raman peak noticed at 1376 cm^{-1} was assigned to Ring1 stretching Carbon–Carbon vibration.

4.3.4. Nitrogen-oxygen, carbon-nitrogen and carbon-oxygen vibrations

In the current study, the nitrogen-oxygen stretching vibrations were noticed in Infrared spectra at 910 cm^{-1} and were compared with theoretical scaled frequency of 928 cm^{-1}. The recognition of Carbon–Nitrogen is a hard assignment since the combination of vibrations is potential in their frequency region. An infrared band spectrum observed at 2035 cm^{-1} compared with theoretical scaled frequency 1902 cm^{-1} was assigned to Carbon–Hydrogen stretching frequency.

4.4. ^{1}H and ^{13}C NMR spectra

The characterization of 3P5I was additionally strengthened by NMR spectroscopy. The Experimental chemical sifts are shown in Fig. 4. The hypothetical chemical shifts of ^{1}H and ^{13}C NMR Spectra were measured using GIAO level at high level basis set. Theoretical chemical shifts were compared with experimental chemical shifts

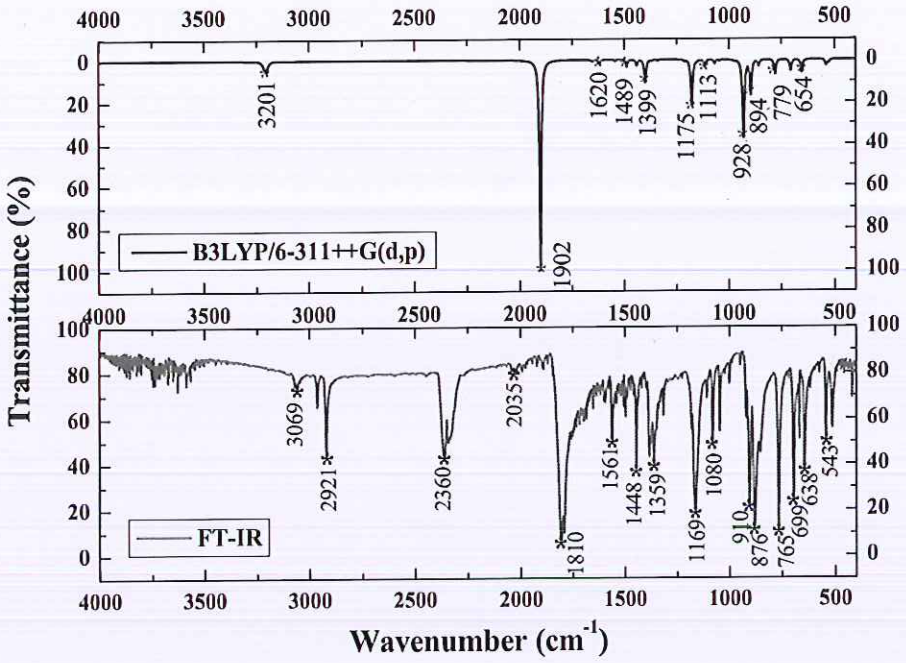

Fig. 2. (a) Experimental, (b) Simulated FT-IR spectra of 3-phenyl-5-isooxazolone

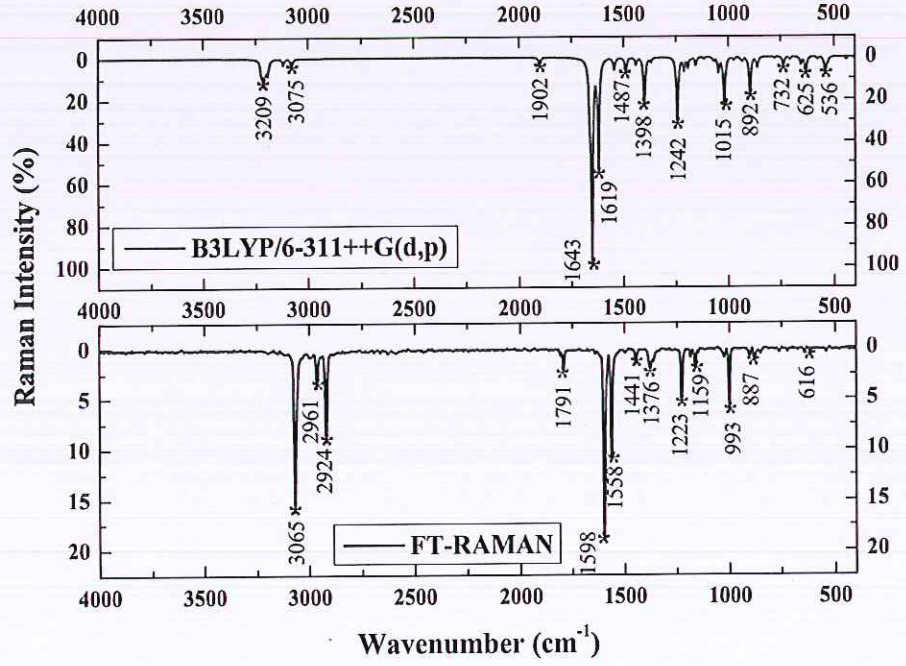

Fig. 3. (a) Experimental and (b) simulated FT-Raman spectra of 3-phenyl-5-isooxazolone

and displayed in Table 3, but they are not in close agreement.

Investigational ^{13}C NMR spectra signal at 161.76 ppm due to C8 atom in the oxazolone ring corresponds to 158.91 ppm. Chemical shift of carbonyl group carbon atom occurs at 27.32 ppm and was computed at 24.84 ppm.The peak at 30.58 ppm is allotted to C7 atom of the oxazolone with computed value32.85 ppm.The aromatic carbon atoms occur in the range 44.90–11.58 ppm and are computed in the range 65.85–126.52 ppm. In the ^{1}H NMR spectrum, the peaks at 6.085 and 6.068 ppm shows the protons (H18 and H19) of the methylene group and the computed values are 5.994 and 5.986 ppm.H13 and H14 protons show a chemical shift at 4.968 and 5.555 ppm and the computed values are at 4.916 and 5.660 ppm.

4.5. UV–vis spectral analysis

This section discusses the result of the theoretical and experimental UV spectra of 3P5I molecule. Experimental spectra were

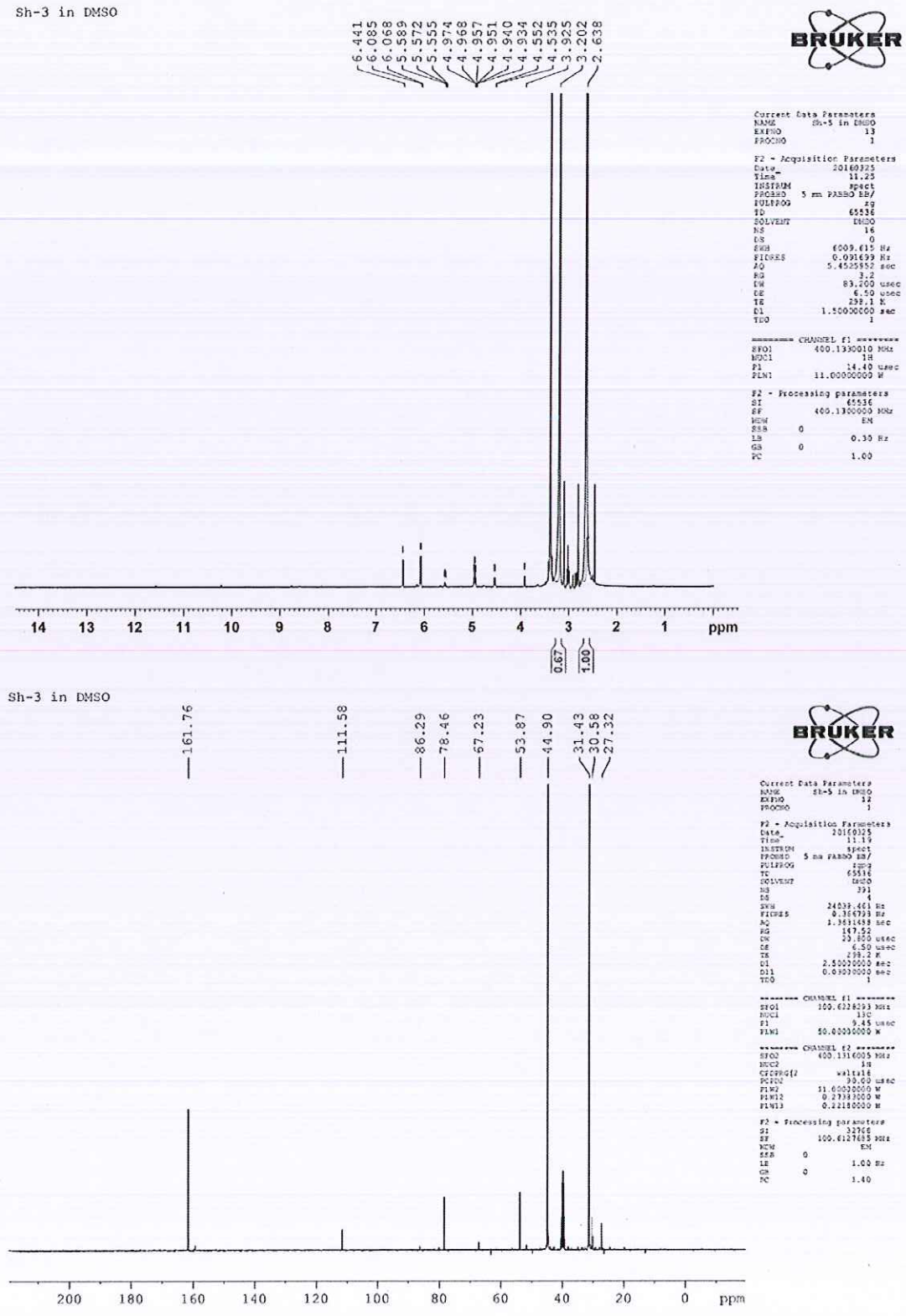

Fig. 4. Experimental a) ^{13}C and b) ^{1}H Chemical shift spectra of 3-Phenyl-5-isooxazolone.

Table 3
Experimental and theoretical 13C and 1H isotropic chemical shifts (ppm) for the **3-phenyl-5-isooxazolone.**

Atom	Experimental (ppm)	Calculated (ppm)
	DMSO	B3LYP 6-311++G(d,p)
C1	44.90	65.85
C2	67.23	68.50
C3	78.46	69.07
C4	111.58	126.52
C5	53.87	66.97
C6	86.29	70.72
C7	30.58	32.85
C8	161.76	158.91
C9	27.32	24.84
H13	4.968	4.916
H14	5.555	5.660
H15	4.940	4.848
H16	4.934	4.842
H17	2.638	2.324
H18	6.085	5.994
H19	6.068	5.986

Note: The atom numbering according to Fig. 1 used in the assignment of chemical shifts.

taken in DMSO solvent and a peak with absorption maxima 263 nm was observed (Fig. 5). Time-Dependent density functional theory simulations can be used to study the light harvesting properties of the compound [18]. The molecule was analyzed for their gas phase excited states using the TD-DFT formalism with CAM-B3LYP functional and the basis set used for the optimization using the DMSO solvent cage as per the IEPCM solvation model. The simulated electronic spectra show that there is a significant peak at 261.23 nm with oscillator strength of 0.653. The experimental and simulated spectra are in very close agreement. The major contributors to this electronic transition are from HOMO to LUMO (96%). There are two possible transitions also at 250.5 and 227 nm, but their oscillator strengths are less than 0.06, hence ignored. Light harvesting efficiency is defined as LHE = $1\text{-}10^{-f}$, where f is the oscillator strength of the electronic transition. For this transition, LHE is 0.7777, which means that the compound presented in the manuscript can convert 77.77% of the absorbed light energy into electronic energy. This compound is hence an ideal candidate to be used as a photosensitiser in Dye Sensitized Solar Cells (DSSC). The vertical electronic excitation energy is 4.74 eV. The excited state frontier orbitals HOMO is at −8.49 eV and LUMO is at −0.868 eV. The energy for electron injection is 3.7459 eV. If the semiconductor used in the DSSC is TiO_2, whose conduction band gap is 4.00 eV, the free energy of electron injection is −5.85973 kcal/mol and it is a very good amount of free energy, which is generated after electron excitation. When compared to a standard cell of output voltage 1.131956 V, JSC 8.72 and fill factor 0.72, our compound when used in titanium based DSSC can provide an cell efficiency of 8.57%, which is a very good amount (Tables 4 and 5).

4.6. Electronic properties

4.6.1. Molecular Electrostatic Potential

For an electrophilic and nucleophilic procedure to hypothesize reactive sites Molecular Electrostatic Potential (MEP) surface scan was obtained at B3LYP functional through high level 6-311++G(d,p) set used for optimized structure of the titled compound. Red and yellow negative MEP regions and blue positive regions corresponding to electrophilic and nucleophilic reactivity sites visualized in Fig. 6. From the figure we noticed that the negative regions for the title molecule were around the oxygen atoms of carbonyl group and the oxygen atom on the oxazolone ring. However, the more negative region is around O12 atom and a positive electrostatic potential area is noticed around the N1 atom of the oxozolone ring. Thus the electrophilic reactive site of the 3P5I molecule is at O11 and O12 positions and the nucleophilic reactive site is at N1 atom. These reactive sites present information regarding the area about bonding and intermolecular interactions.

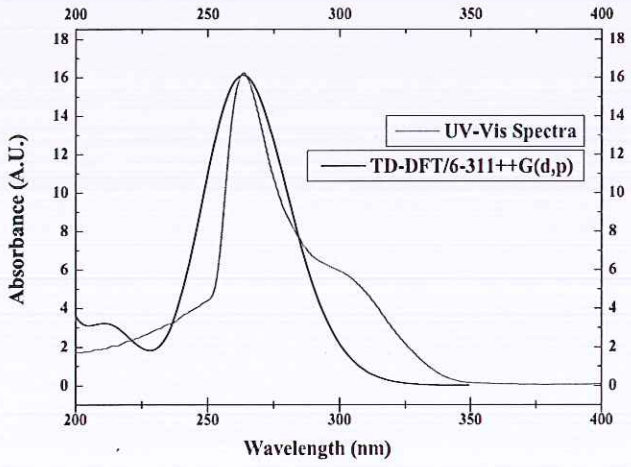

Fig. 5. Theoretical and experimental UV/Vis spectra of 3-phenyl-5-isooxazolone

Table 5
Photovoltaic modelling of the compound using TD-DFT (CAM-B3LYP/6-311++G**).

f	0.6530
LHE	0.777669
λ(max) (nm)	261.23
E(0,0) (eV)	4.746775
E(HOMO) (au)	−0.3121
E(HOMO) (eV)	−8.49268
E(LUMO) (au)	−0.0319
E(LUMO) (eV)	−0.86804
Eg (au)	0.2802
Eg (eV)	7.624634
Edye (eV)	8.492678
E*dye (eV)	3.745903
E(CB) (eV)	−4
ΔGinject (eV)	−0.2541
ΔGinject (kJ/mol)	−24.5165
ΔGinject (kcal/mol)	−5.85973
Voc(V)	1.131956
Jsc (mAcm^2)	8.72
FF	0.72
η(%)	8.572828

Table 4
The UV–Vis excitation energy and oscillator strength of 3-phenyl-5-isooxazolone by TD-DFT/B3LYP/6-311++G (d, p) method.

No.	Exp. Wavelength	Energy (cm-1)	Wavelength (nm)	Osc. Strength	Symmetry	Major contribs
1	–	37631.4099939	265.7354588	0.0011	Singlet-A	H-2->LUMO (93%)
2	263 nm	37762.8783658	264.810322538	0.2987	Singlet-A	H-1->LUMO (14%), HOMO->LUMO (80%)
3	–	48392.4591856	206.64376575	0.0064	Singlet-A	H-3->LUMO (22%), H-1->L+1 (15%), HOMO->L+2 (58%)

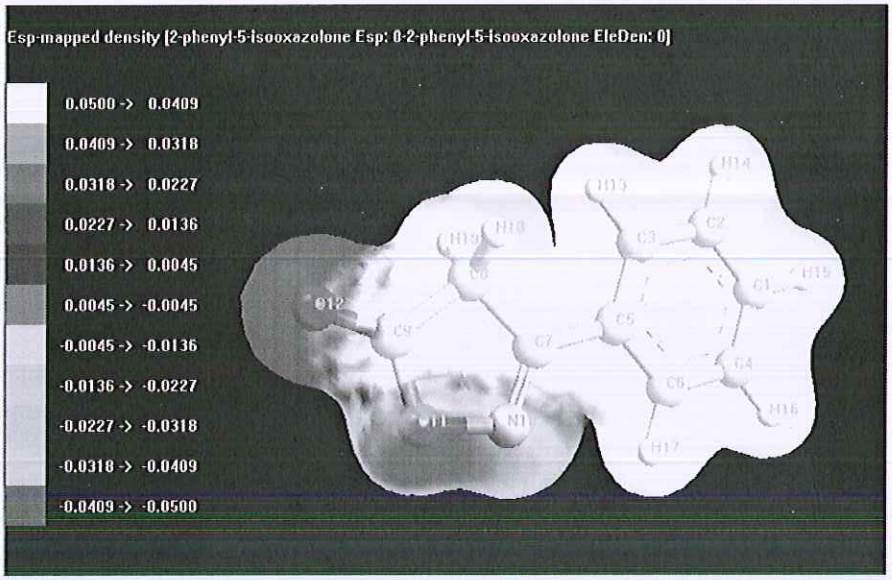

Fig. 6. 3D-View molecular electrostatic potential of 3-phenyl-5-isooxazolone

Hence from the figure, the intermolecular interactions exist at C9-O12 and N1-O11 bonds.

4.6.2. Frontier molecular orbitals

By investigating the frontier orbitals of an organic compound the process of reaction with another molecule and the optical properties can be determined. The atomic orbital components visualization of frontier molecular orbital in Ground state HOMO-42 and the first excited state LUMO-43 of 3P5I is shown in Fig. 7 and the multiple surfaces of HOMO-42 and LUMO-43 are visualized in Fig. 8. The HOMO-LUMO energy separation value is 4.9756eV.This large HOMO–LUMO gap meant good stability, excitation energy is large for excited energy levels and chemical hardness is enormous for 3P5I molecule.

4.6.3. Chemical reactivity descriptors

The Chemical reactivity Descriptors of 3P5I were noticed byB3LYP/6-311++G (d,p) approach. The parameters like Ionization

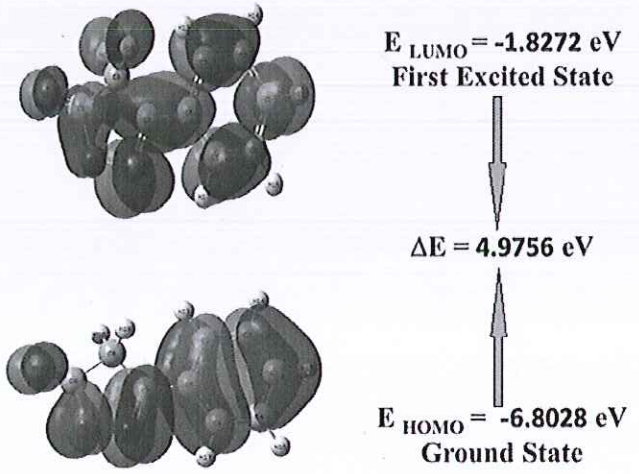

Fig. 7. Ground state (HOMO: 42) and First exited state (LUMO: 43) Visualization of 2-phenyl-5-isooxazolone

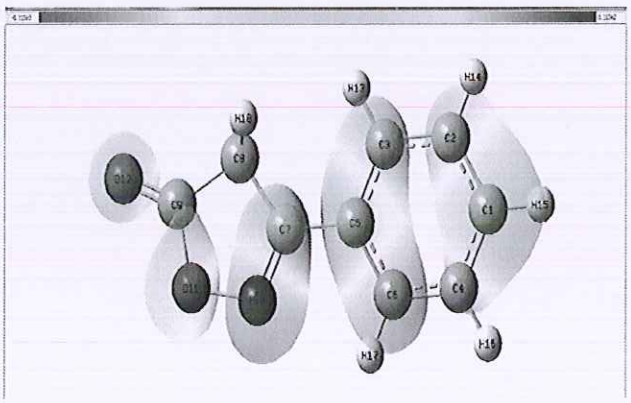

Fig. 8. Multiple surfaces HOMO: 42 and LUMO: 43 of 3-phenyl-5-isooxazolone

potential (I), Electron Affinity (A), Chemical potential (μ), Electronegativity (χ), Chemical hardness (η), Electrophilicity index (ω) and Global Softness (σ) were calculated with the support of Koopmans's theorem [19–21].

$$\text{Ionization potential (I)} = -E_{HOMO} \quad (2)$$

$$\text{Electron Affinity (A)} = -E_{LUMO} \quad (3)$$

$$\text{Chemical potential } (\mu)\ (\text{eV}) = -\frac{1}{2}\left(E_{HOMO} + E_{LUMO}\right) \quad (4)$$

$$\text{Electronegativity } \chi = I + \frac{A}{2} \quad (5)$$

$$\text{Chemical hardness } \eta = I - \frac{A}{2} \quad (6)$$

$$\text{Electrophilicity index } \omega = \frac{\mu^2}{2\eta} \quad (7)$$

$$\text{Global Softness } \sigma = \frac{1}{\eta} \quad (8)$$

The computed Ionization potential (I) and the Electron affinity (A) of compound are 6.802eV and 1.827eV. The computed chemical reactivity descriptors were listed in Table 6. High chemical Hardness (5.889) of the compound shows the toughness of the compound. These properties reveal 3P5I is a biologically active compound.

4.6.4. Natural bond orbital analysis

To investigate the donor acceptor interaction for 3P5I compound Second-order perturbation theory analysis of Fock matrix in the NBO basis is listed by DFT approach in Table 7. TheNBO donor i and NBO acceptor j and the $E^{(2)}$stabilization energy can be represented by

$$E^{(2)} = -n_\sigma \frac{\langle \sigma | F | \sigma \rangle^2}{\varepsilon_\sigma^* - \varepsilon_\sigma} = -n_\sigma \frac{F_{ij}^2}{\Delta E} \quad (9)$$

Here F^2_{ij} are i, j matrix elements of orbitals, $\varepsilon_\sigma, \varepsilon_\sigma^*$ were natural bond orbitals energies(σ, σ^*) and n_σ was donor orbital population. Large value of $E^{(2)}$denotes the great transferring tendency from electron donors to acceptors which measures the conjugation of the entire compound. The great intramolecular hyperconjugative interaction of σ, π electrons of Carbon–Carbon with anti-bond Carbon–Carbon affects the stabilization of the molecule in the ring structure. In the table, π (C3-C5) distributes to π^*(C1-C2) and π^*(C4-C6) of stabilization energy 18.95 and 18.66 kJ mol^{-1}respectively. Similarly, π (C1-C2) distributes to π^*(C3-C5) and π^*(C4-C6) and σ (C4-C6) distributes to π^*(C1-C2) and π^*(C3-C5) shows high stabilization energy. Further significant intramolecular hyperconjugative interaction is acquired from LP → π^* transition. The Lone pair interactions of LP O11 → π^* (C9–O12) and LP O12 → π^* (C9–O11) shows stabilization energy at 42.85 and 38.38 kJ mol^{-1} respectively. From NBO study results the rate of high interactions meant for suggesting bioactive nature of the compound.

4.6.5. NLO (non-linear optical properties)

NLO properties of 3P5I compound were studied using DFT/B3LYP/6-311++G (d,p) basis set are shown in Table 8. The dipole moment (μ), the mean first hyperpolarizability (β), the mean polarizability (α_0), the anisotropy of polarizability ($\Delta\alpha$) using x,y,z(Cartesian)coordinates can be computed by using Gaussian 09W in the finite-field approach is represented in Table 9 and equated as follows [22,23].

$$\mu = \mu_x^2 + \mu_y^2 + \mu_z^2 \quad (10)$$

$$\alpha_o = \frac{\alpha_{xx} + \alpha_{yy} + \alpha_{zz}}{3} \quad (11)$$

$$\Delta\alpha = 2^{-1/2}[(\alpha_{xx} - \alpha_{yy})^2 + (\alpha_{yy} - \alpha_{xx})^2 + 6\alpha_{xx}^2]^{1/2} \quad (12)$$

$$\beta = (\beta_x^2 + \beta_y^2 + \beta_z^2)^{1/2} \quad (13)$$

$$\beta_x = \beta_{xxx} + \beta_{xyy} + \beta_{xzz} \quad (14)$$

$$\beta_y = \beta_{yyy} + \beta_{xxy} + \beta_{yzz} \quad (15)$$

$$\beta_z = \beta_{zzz} + \beta_{xxz} + \beta_{yyz} \quad (16)$$

The constants $\alpha_o$and β mean from Gaussian 09 W Revision- D.01 program in atomic units (a.u) were to be converted into electrostatic units (esu) (for α: 1a.u = 0.1482 × 10^{-12} esu and for β: 1 a.u = 8.6393 × 10^{-33} esu). The values of the mean first hyperpolarizability (β) and the mean polarizability (α_0) of 3P5I compound calculated as 0.685029 × 10^{-30} esu and 14.21879 × 10^{-24} esu respectively. The μ along z direction is 0.631199 D which indicates atomic charges non-uniform distribution.

4.6.6. Mulliken atomic charges

The atomic charges were calculated by MPA (Mulliken Population Analysis) from DFT approach high level basis set are represented at Table 8. The graphical Mulliken atomic charges were shown in Fig. 9. The Mulliken atomic charges play an essential role to determine the biological activity of the title molecule. All the hydrogen (H13, H14, H15, H16, H17, H18 and H19) atoms have positive charges. Some carbon (C1, C2, C3, C4, C6, and C8) atoms have negative charges which are bonded with hydrogen atoms. Remaining carbon atoms (C5, C7, and C9) has positive atomic charge values. In the gas phase N10,O11 and O12 atoms have more negative atomic charges. MPA confirms the carbon-hydrogen-oxygen intramolecular interactions of 3P5I compound in solid phase.

4.6.7. Molecular docking studies

Molecular docking studies involve two steps. First step is the Prediction of Activity Spectra (PASS) which is used to predict the biological activity of a compound [24]. In the second step, the detailed docking analysis of the activity predicted from PASS data is performed [25–31]. The PASS was performed using a commonly used online tool. PASS analysis prediction of the compound is given in Table 10.

We chose two activities apoptosis agonist and antiasthmatic with probability to be active (Pa) values are 0.873 and 0.863 and the corresponding proteins BCL2L10 (apoptosis facilitator)(PDB ID: 6FBX) and Trypsinogen(1NC6) (antiasthmatic) downloaded from the protein data bank website. All molecular docking calculations were performed on Auto Dock-Vina software [25]. The detailed interactions of ligand with receptors are shown in Figs. 9 and 10. The docked ligand forms stable complexes with corresponding receptors BCL2L10 and Trypsinogen in Figs. 11 and 12. The binding affinity (ΔG in kcal/mol) value of compound with receptor BCL2L10 and Trypsinogen are −5.4 and −5.2as tabulated in Tables 11 and 12. These preliminary results suggest that the compounds might

Table 6
The calculated quantum chemical activity descriptors parameters of **3-phenyl-5-isooxazolone**.

Property	2-phenyl-5-isooxazolone
Total energy (eV)	−15029.9842605
E_{HOMO} (eV)	−6.80284975
E_{LUMO} (eV)	−1.82724544
Energy gap (ΔE) (eV)	4.97560431
Ionization potential (I) eV	6.80284975
Electron Affinity (A) eV	1.82724544
Electro-negativity (χ)eV	7.71647247
Chemical Potential (μ)	4.315047595
Chemical hardness(η)eV	5.88922703
Electrofilicity index (ω)eV	1.580821698
Global Softness (σ)eV	0.169801571
Dipole moment(D)	5.451642

Table 7
Second order perturbation theory analysis of fock matrix in NBO basis for 3-phenyl-5-isooxozolone.

Donor (i)	Type	Ed/e	Acceptor (j)	Type	Ed/e	$E^{(2)a}$ (kJ mol^{-1})	E(i)-E(j)[b] (a.u)	f(I,j)[c] (a.u)
C1-C2	σ	1.98112	C1-C4	σ*	0.01588	2.35	1.27	0.049
	σ	1.98112	C2-C3	σ*	0.01430	2.55	1.27	0.051
	σ	1.98112	C3-H13	σ*	0.01238	2.38	1.16	0.047
	σ	1.98112	C4-H16	σ*	0.01207	2.25	1.18	0.046
C1-C2	π	1.65322	C3-C5	π*	0.38313	21.29	0.28	0.069
	π	1.65322	C4-C6	π*	0.28641	18.46	0.29	0.066
C1-C4	σ	1.98133	C1-C2	σ*	0.01552	2.37	1.27	0.049
	σ	1.98133	C1-C4	σ*	0.01588	2.50	1.28	0.051
	σ	1.98133	C6-H17	σ*	0.01284	2.30	1.18	0.047
C1-H15	σ	1.98296	C2-C3	σ*	0.01430	3.63	1.10	0.056
	σ	1.98296	C4-C6	σ*	0.01411	3.53	1.11	0.056
C2-C3	σ	1.97994	C1-H15	σ*	0.01197	2.26	1.18	0.046
	σ	1.97994	C3-C5	σ*	0.02167	3.07	1.26	0.056
	σ	1.97994	C5-C7	σ*	0.03403	3.41	1.18	0.056
C2-H14	σ	1.98247	C1-C4	σ*	0.01588	3.53	1.10	0.056
	σ	1.98247	C3-C5	σ*	0.02167	3.85	1.09	0.058
C3-C5	σ	1.97481	C2-C3	σ*	0.01430	2.58	1.27	0.051
	σ	1.97481	C5-C6	σ*	0.02264	3.80	1.26	0.062
	σ	1.97481	C5-C7	σ*	0.03403	2.49	1.18	0.048
C3-C5	π	1.64762	C1-C2	π*	0.31815	18.95	0.29	0.066
	π	1.64762	C4-C6	π*	0.28641	18.66	0.29	0.067
	π	1.64762	C7-N10	π*	0.17309	20.02	0.27	0.068
C3-H13	σ	1.98180	C1-C2	σ*	0.31815	3.47	1.11	0.055
	σ	1.98180	C5-C6	σ*	0.01588	4.07	1.09	0.060
C4-C6	σ	1.98030	C1-C4	σ*	0.01588	2.46	1.27	0.050
	σ	1.98030	C5-C6	σ*	0.02264	2.85	1.26	0.054
	σ	1.98030	C5-C7	σ*	0.03403	3.49	1.18	0.057
C4-C6	π	1.66339	C1-C2	π*	0.31815	20.68	0.28	0.068
	π	1.66339	C3-C5	π*	0.38313	19.73	0.28	0.067
C4-H16	σ	1.98237	C1-C2	σ*	0.01552	3.53	1.10	0.056
	σ	1.98237	C5-C6	σ*	0.01588	3.91	1.08	0.058
C5-C6	σ	1.97326	C3-C5	σ*	0.02167	3.86	1.25	0.062
	σ	1.97326	C5-C7	σ*	0.03403	2.59	1.17	0.049
	σ	1.97326	C7-C8	σ*	0.02805	2.76	1.09	0.049
C5-C7	σ	1.96953	C5-C6	σ*	0.02264	2.35	1.24	0.048
	σ	1.96953	N10-O11	σ*	0.02950	3.45	0.88	0.049
C6-H17	σ	1.98062	C1-C4	σ*	0.01588	3.68	1.09	0.057
	σ	1.98062	C3-C5	σ*	0.02167	4.25	1.08	0.061
C7-C8	σ	1.97666	C9-O12	σ*	0.01345	5.08	1.29	0.072
C7-N10	σ	1.99074	C5-C7	σ*	0.03403	2.04	1.39	0.048
C7-N10	π	1.94411	C3-C5	σ*	0.38313	8.09	0.37	0.053
	π	1.94411	C8-H18	σ*	0.01104	2.50	0.77	0.040
	π	1.94411	C8-H19	σ*	0.01104	2.50	0.77	0.040
C8-C9	σ	1.98380	C5-C7	σ*	0.03403	4.96	1.13	0.067
C8-H18	σ	1.95644	C7-N10	σ*	0.17309	3.88	0.55	0.042
	σ	1.95644	C9-O12	σ*	0.20752	4.17	0.55	0.044
C8-H19	σ	1.95639	C7-N10	σ*	0.17309	3.89	0.55	0.043
	σ	1.95639	C9-O12	σ*	0.20752	4.18	0.55	0.045
N10-O11	σ	1.98131	C5-C7	σ*	0.03403	4.83	1.28	0.070
	σ	1.98131	C9-O12	σ*	0.01345	3.87	1.43	0.066
LP								
N10	LP	1.95219	C7-C8	σ*	0.02805	7.01	0.84	0.069
	LP	1.95219	C9-O11	σ*	0.12938	4.94	0.77	0.056
O11	LP	1.76640	C7-N10	π*	0.17309	14.69	0.34	0.064
	LP	1.76640	C9-O12	π*	0.01345	42.85	0.34	0.108
O12	LP	1.82296	C8-C9	π*	0.07646	21.44	0.61	0.105
	LP	1.82296	C9-O11	π*	0.12938	38.38	0.58	0.135

[a] $E^{(2)}$ means energy of hyper conjugative interaction (stabilization energy).
[b] Energy difference between donor and acceptor i and j NBO orbitals.
[c] F(i, j) is the Fock matrix element between i and j NBO orbitals.

exhibit inhibitory activity against receptors [32–37] (see Fig. 13).

5. Conclusions

The isooxazolone derivative was studied extensively using experimental and theoretical tools. The computational and experimental scaled IR and Raman spectra showed close agreement. Detailed vibrational assignments and potential energy distribution was also performed inorder to explain the IR and Raman spectra. Also, the experimental and simulated NMR spectra were also in agreement and they were highly useful in reaching the exact structure of the compound. The simulated and experimental UV spectra in DMSO also showed close agreement. The TD-DFT simulated UV spectra was used to explain the various transitions and the

Table 8
The electric dipole moment μ(D) the average polarizability α_{tot} (× 10^{-12} esu) and the first hyperpolarizability β_{tot} (× 10^{-30} esu) of **3-phenyl-5-isooxazolone** by HF/6-311++G (d,p) method.

μ and α components	B3LYP/6-311++G(d,p)	β components	B3LYP/6-311++G(d,p)
μ_x	−2.5332144	β_{xxx}	−47.0307177
μ_y	0.0035989	β_{xxy}	−0.0037324
μ_z	−0.6311991	β_{xyy}	−19.0107595
μ(D)	6.81560042	β_{yyy}	0.386324
α_{xx}	134.0059369	β_{xxz}	43.6245166
α_{xy}	−0.0325465	β_{xyz}	0.0620017
α_{yy}	41.3137003	β_{yyz}	12.7825136
α_{xz}	20.2638948	β_{xzz}	−5.0799961
α_{yz}	0.1146076	β_{yzz}	−0.0440249
α_{zz}	112.5140165	β_{zzz}	−21.3480793
Δα	37.039003 × 10^{-24} esu		
α_0(esu)	14.21879 × 10^{-24}	β total (esu)	0.685029 × 10^{-30}

Table 9
Atomic charges for optimized geometry of 3-phenyl-5-isooxazolone

S.No.	Atom	Mulliken
1	C	−0.07461
2	C	−0.09024
3	C	−0.13248
4	C	−0.09086
5	C	0.102342
6	C	−0.10237
7	C	0.26813
8	C	−0.37143
9	C	0.64193
10	N	−0.20789
11	O	−0.37131
12	O	−0.45371
13	H	0.084575
14	H	0.10275
15	H	0.109733
16	H	0.107109
17	H	0.123176
18	H	0.177524
19	H	0.177611

Table 10
PASS prediction for the activity spectrum of test compound. Pa represents probability to be active and Pi represents probability to be inactive.

Pa	Pi	Activity
0.874	0.004	Antiallergic
0.873	0.005	Apoptosis agonist
0.863	0.005	Antiasthmatic
0.860	0.005	Antiinflammatory
0.861	0.014	Phobic disorders treatment
0.854	0.019	Aspulvinonedimethylallyltransferase inhibitor
0.804	0.013	Glycosylphosphatidylinositol phospholipase D inhibitor
0.797	0.008	Glucan endo-1,6-beta-glucosidase inhibitor
0.779	0.009	Complement factor D inhibitor
0.779	0.010	Pullulanase inhibitor
0.774	0.010	CarboxypeptidaseTaq inhibitor
0.768	0.013	Dehydro-L-gulonate decarboxylase inhibitor
0.748	0.009	Creatininase inhibitor
0.776	0.041	Membrane integrity agonist

oscillator strength of the major electronic transition is such that the light harvesting efficiency of the compound is used in a DSSC was found to be 77%. When compared with a standard experimental cell with standard photosensitisers, if this compound was used as the photosensitiser, the photovolatic efficiency was found to be 8.57% in titanium based cells which is not a bad efficiency value. NBO studies could explain the various hyperconjugative interactions in the molecule. NLO property analysis shows that the compound is a

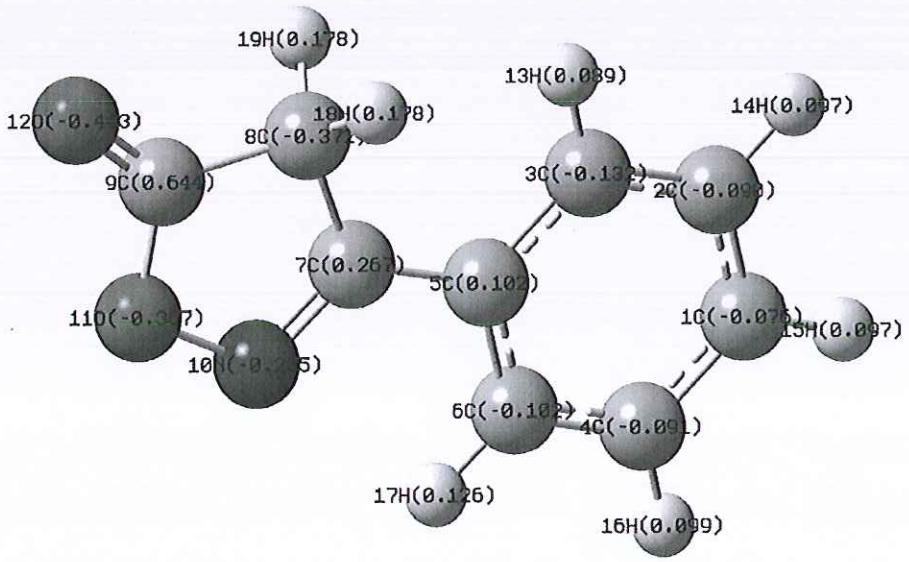

Fig. 9. Graphical Mulliken atomic charge distribution of **3-phenyl-5-isooxazolone** obtained from B3LYP/6-311++G (d,p).

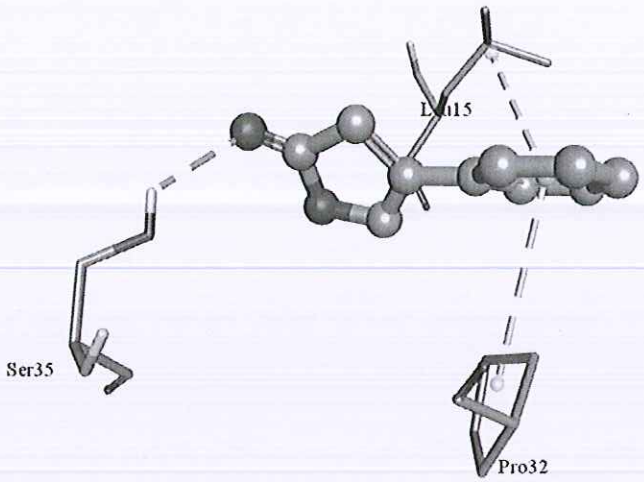

Fig. 10. Interactive plot of ligand with the amino acids of BCL2L10.

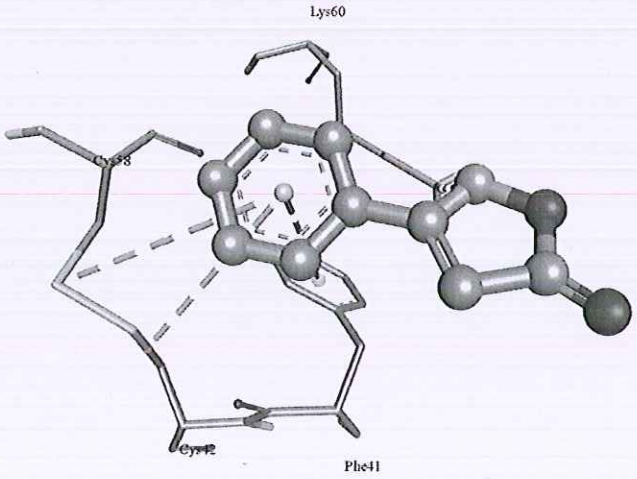

Fig. 11. Interactive plot of ligand with the amino acids of Trypsinogen.

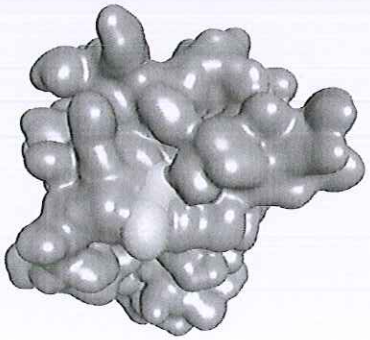

Fig. 12. Schematic for the ligand (red) at the active site of BCL2L10.

very good non linear material when compared to the standard material urea. Also docking studies indicates that the compounds are having anticancer and antiasthmatic effects.

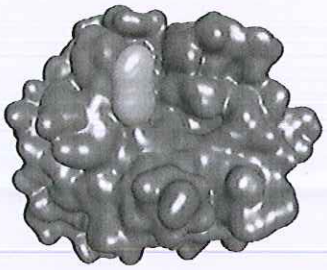

Fig. 13. Schematic for the ligand (yellow) at the active site of Trypsinogen.

Table 11
The binding affinity values of different poses of the title compound with BCL2L10 (apoptosis facilitator) predicted by Autodock Vina.

Mode	Affinity (kcal/mol)	Distance from best mode (Å)	
–	–	RMSD l.b.	RMSD u.b.
1	−5.4	0.000	0.000
2	−5.3	14.795	15.612
3	−5.2	14.124	16.235
4	−5.2	18.821	20.445
5	−5.0	13.405	14.791
6	−5.0	13.639	14.895
7	−4.8	4.950	6.399
8	−4.7	16.109	18.305
9	−4.7	16.647	17.535

Table 12
The binding affinity values of different poses of the title compound with Trypsinogenpredicted by AutodockVina.

Mode	Affinity (kcal/mol)	Distance from best mode (Å)	
–	–	RMSD l.b.	RMSD u.b.
1	−5.2	0.000	0.000
2	−5.1	7.399	9.135
3	−5.1	2.076	2.357
4	−5.0	17.511	18.887
5	−5.0	8.574	10.032
6	−4.8	3.373	4.087
7	−4.8	1.737	2.611
8	−4.7	6.670	8.788
9	−4.7	3.325	4.265

Author's contribution

All authors contributed equally to the manuscript.

Declaration of competing interest

Authors do not report any conflicts of interests.

Acknowledgements

The authors are appreciative to SAIF, IIT Madras and NMR Spectroscopy Laboratories Andhra University for Experimental studies. The authors are thankful to Molvib program by T. Sindius.

Appendix A. Supplementary data

Supplementary data to this article can be found online at https://doi.org/10.1016/j.molstruc.2019.127461.

References

[1] V. Smokal, R. Czaplicki, B. Derkowska, O. Krupka, A. Kolendo, B. Sahraoui, Synthesis and study of nonlinear optical properties of oxazolone containing polymers, Synth. Met. 157 (2007) 708–712.

[2] H.C. Song, Y.F. Sun, W.M. Li, Z.L. Xu, L.Z. Zhang, Z.G. Cai, Second nonlinear polarizability of 4- substituted - benzylideneoxazol- 5(4 H) - ones and 9-substituted- phenylaeridines, Acta Chim. Sin. 59 (2001) 1563–1565.

[3] H.C. Song, H. Wen, W.M. Li, Study on the second-order optical behavior of 4-(substituted-benzylidene)-2-phenyl-4*H*-oxazol-5-one, Spectrochim. Acta A Mol. Biomol. Spectrosc. 60 (2004) 1587–1591.

[4] J.L. Diaz, B. Villacampa, F. Lopez-Calahorra, D. Velasco, Experimental and theoretical study of a new class of acceptor group in chromophores for nonlinear optics: 2- substituted 4- methylene-4H-oxazol-5-ones, Chem. Mater. 14 (2002) 2240–2251.

[5] H.C. Song, H. Wen, W.M. Li, Study on the second-order optical behavior of 4-(substituted-benzylidene)-2-phenyl-4H-oxazol-5-one, Spectrochim. Acta: Molecular and Biomolecular Spectroscopy 60 (2004) 1587–1591.

[6] R. Thomas, Y.S. Mary, K.S. Resmi, B. Narayana, B.K. Sarojini, S. Armakovic, S.J. Armakovic, G. Vijayakumar, C. Van Alsenoy, B.J. Mohan, Synthesis and spectroscopic study of two new pyrazole derivatives with detailed computational evaluation of their reactivity and pharmaceutical potential, J. Mol. Struct. 1181 (2019) 599–612.

[7] Y.L.N. Murthy, V. Christopher, U.V. Prasad, P.B. Bisht, D.V. Ramanaih, B.S. Kalanoor, et al., Synthesis and study of nonlinear optical properties of 4-substituted benzylidene-2-phenyl oxazol-5-ones by Z-scan technique, Synth. Met. 160 (2010) 535–539.

[8] B. Derkowska, O. Krupka, V. Smokal, B. Sahraoui, Optical properties of oxazalone derivatives with and without DNA-CTMA, Optical Materilas 33 (2011) 1429–1433.

[9] Y.F. Sun, Y.P. Cui, The synthesis, structure and spectroscopic properties of novel oxozolone, pyrazolone and pyrazoline containing heterocyclechromophores, Dyes Pigments 81 (2009) 27–34.

[10] M.J. Frisch, G.W. Trucks, H.B. Schlegel, G.E. Scuseria, M.A. Robb, J.R. Cheeseman, G. Scalmani, V. Barone, B. Mennucci, G.A. Petersson, H. Nakatsuji, M. Caricato, X. Li, H.P. Hratchian, A.F. Izmaylov, J. Bloino, G. Zheng, J.L. Sonnenberg, M. Hada, M. Ehara, K. Toyota, R. Fukuda, J. Hasegawa, M. Ishida, T. Nakajima, Y. Honda, O. Kitao, H. Nakai, T. Vreven, J.A. Montgomery Jr., J.E. Peralta, F. Ogliaro, M. Bearpark, J.J. Heyd, E. Brothers, K.N. Kudin, V.N. Staroverov, T. Keith, R. Kobayashi, J. Normand, K. Raghavachari, A. Rendell, J.C. Burant, S.S. Iyengar, J. Tomasi, M. Cossi, N. Rega, J.M. Millam, M. Klene, J.E. Knox, J.B. Cross, V. Bakken, C. Adamo, J. Jaramillo, R. Gomperts, R.E. Stratmann, O. Yazyev, A.J. Austin, R. Cammi, C. Pomelli, J.W. Ochterski, R.L. Martin, K. Morokuma, V.G. Zakrzewski, G.A. Voth, P. Salvador, J.J. Dannenberg, S. Dapprich, A.D. Daniels, O. Farkas, J.B. Foresman, J.V. Ortiz, J. Cioslowski, D.J. Fox, Gaussian 09, Revision B.01, Gaussian, Inc., Wallingford CT, 2009.

[11] T. Sundius, Molvib - a flexible program for force field calculations, J. Mol. Struct. 218 (1990) 321–326.

[12] T. Sundius, Scaling of ab initio force fields by MOLVIB, Vib. Spectrosc. 29 (2002) 89–95.

[13] S. Margutti, D. Schollmeyer, Stefan laufer,5-dihydroisoxazol-3-yl]-1-methylpyridinium iodide–4-[3-(4-fluorophenyl)-2-methyl-5-oxo-2,5-dihydroisoxazol-4-yl]-1-methylpyridinium iodide (0.6/0.4), Actacrystallographica Section E 64 (2008) 0298–0299.

[14] G. Fogarasi, X. Zhou, P.W. Taylor, P. Pulay, The calculation of ab initio molecular geometrics: efficient optimization by natural internal coordinates and empirical correction by offset forces, J. Am. Chem. Soc. 114 (1992) 8191–8201.

[15] N. Okulik, A.H. Jubert, Theoretical analysis of the reactive sites of non–steroidal anti–inflammatory drugs, Internet Electron. J. Mol. Des. 4 (2005) 17–30.

[16] N.B. Colthup, L.H. Daly, S.E. Wiberley, Introduction to Infrared and Raman Spectroscopy, Academic Press Inc., London, 1964.

[17] G. Socrates, Infrared Characteristic Group Frequencies, John Wiley and sons, GB, 1980.

[18] **D.A. Thadathil, S. Varghese, K.B. Akshaya, R. Thomas, A. Varghese, "An insight into photophysical investigation of (E)-2-Fluoro-N'-(1-(4-Nitrophenyl) Ethylidene)Benzohydrazide through solvatochromism approaches and computational studies, J. Fluoresc. 29 (2019) 1013–1027,** https://doi.org/10.1007/s10895-019-02415-y.

[19] P. Politzer, J.S. Murray, The electrostatic potential: an overview, Wiley Interdisciplinary Reviews: Computational Molecular Science 1 (2011) 153–163.

[20] A.M. Palefox, Scaling factors for the prediction of vibrational spectra. I. Benzene molecule, Int. J. Quantum Chem. 77 (2000) 661–684.

[21] J.S. Al-otaibi, Y.S. Mary, Y.S. Mary, R. Thomas, Quantum mechanical and photovoltaic studies on the cocrystals of hydrochlorothiazide with isonazid and malonamide, J. Mol. Struct. 1197 (2019) 719–726.

[22] P. Karamanis, C. Pouchan, G. Maroulis, Structure, stability, dipole polarizability and differential polarizability in small gallium arsenide clusters from all-electron *ab initio* and density-functional-theory calculations, Phys. Rev. A 77 (2008), 013201.

[23] Y.S. Mary, P.B. Miniyar, Y.S. Mary, K.S. Resmi, S.J. Armakovic, R. Thomas, C.Y. Panicker, S. Armakovic, J. Mol. Struct. 1173 (2018) 469–480.

[24] A. Lagunin, A. Stepanchikova, D. Filimonov, V. Poroikov, PASS: prediction of activity spectra for biologically active substances, Bioinformatics 16 (2000) 747–748.

[25] O. Trott, A.J. Olson, AutoDockVina: improving the speed and accuracy of docking with a new scoring function, efficient optimization and multithreading, J. Comput. Chem. 31 (2010) 455–461.

[26] R. Thomas, Y.S. Mary, K.S. Resmi, B. Narayana, B.K. Sarojini, G. Vijayakumar, C. Van Alsenoy, Two neoteric pyrazole compounds as potential anti-cancer agents:synthesis, electronic structure, physic-chemical properties and docking analysis, J. Mol. Struct. 1181 (2019) 455–466.

[27] M. Hossain, R. Thomas, Y.S. Mary, K.S. Resmi, S. Aramkovic, S.J. Armakovic, A.K. Nanda, G. Vijayakumar, C. VanAlsenoy, Understanding reactivity of two nearly synthetized imidazole derivatives by spectroscopic characterization and computational study, J. Mol. Struct. 1158 (2018) 176–196.

[28] **S. Beegum, Y.S. Mary, Y.S. Mary, R. Thomas, S. Armaković, S.J. Armaković, J. Zitko, M. Dolezal, C. Van Alsenoy, Exploring the detailed spectroscopic characteristics, chemical and biological activity of two cyanopyrazine-2-carboxamide derivatives using experimental and theoretical tools, Spectrochim. Acta Part A: Molecular and Biomol Spectroscopy 224 (2020) 117414,** https://doi.org/10.1016/j.saa.2019.117414.

[29] P.R.K. Rani, Y.S. Mary, A. Fernandez, S.A. Priya, Y.S. Mary, R. Thomas, Single crystal XRD, DFT investigations and molecular docking study of 2-((1,5-dimethyl-3-oxo-2-phenyl-2,3-dihydro-1H-pyrazol-4-yl)amino)naphthalene-1,4-dione as a potential anti-cancer lead molecule, Comput, Biol. Chem. 78 (2019) 153–164.

[30] Y.S. Mary, P.B. Miniyar, Y.S. Mary, K.S. Resmi, C.Y. Panicker, S. Armakovic, S.J. Armakovic, R. Thomas, B. Sureshkumar, Synthesis and spectroscopic study of three new oxadiazole derivatives with detailed computational evaluation of their reactivity and pharmaceutical potential, J. Mol. Struct. 1173 (2018) 469–480.

[31] **Y. S Mary, C.Y. Panicker, R. Thomas, B. Narayana, S. Samshuddin, B.K. Sarojini, S. Armaković, S.J. Armaković, G.G. Pillai, Theoretical studies on the structure and various physico-chemical and biological properties of a terphenyl derivative with immense anti-protozoan activity, Polycycl. Aromat. Compd. (2019),** https://doi.org/10.1080/10406638.2019.1624974.

[32] **S. Beegum, Y.S. Mary, Y.S. Mary, R. Thomas, S. Armaković, S.J. Armaković, J. Zitko, M. Dolezal, C. Van Alsenoy, Exploring the detailed spectroscopic characteristics, chemical and biological activity of two cyanopyrazine-2-carboxamide derivatives using experimental and theoretical tools, Spectrochim. Acta: Molecular and Biomol Spectroscopy 224 (2020) 117414,** https://doi.org/10.1016/j.saa.2019.117414.

[33] V. S Kumar, Y. S Mary, K. Pradhan, D. Brahman, Y. S Mary, R. Thomas, M.S. Roxy, C. Van Alsenoy, Synthesis , spectral properties , chemical descriptors and light harvesting studies of a new bioactive Azo imidazole compound, J. Mol. Struct. 1199 (2020) 127035.

[34] A.A. Al-saadi, Conformational pro fi le , vibrational assignments , NLO properties and molecular docking of biologically active, Heliyon 5 (2019) e01987. December 2018.

[35] D. Majumdar, S. Das, R. Thomas, Z. Ullah, S.S. Sreejith, Syntheses , X-ray crystal structures of two new Zn (II) -dicyanamide complexes derived from H 2 vanen-type compartmental ligands : investigation of thermal , photoluminescence , in vitro cytotoxic e ff ect and DFT-TDDFT studies, Inorg. Chim. Acta 492 (April) (2019) 221–234.

[36] **J. S. Al-Otaibi, Y. S. Mary, S. Armaković, and R. Thomas, "Hybrid and bioactive cocrystals of pyrazinamide with hydroxybenzoic acids: detailed study of structure, spectroscopic characteristics, other potential applications and noncovalent interactions using SAPT," J. Mol. Struct. 127316, 2020.**

[37] Y.S. Mary, Y.S. Mary, K.S. Resmi, R. Thomas, Heliyon DFT and molecular docking investigations of oxicam derivatives, Heliyon 5 (June) (2019) e02175.